Vol. 555: 109–123, 2016
doi: 10.3354/meps11828

MARINE ECOLOGY PROGRESS SERIES
Mar Ecol Prog Ser

Published August 18

A longitudinal study of Pacific oyster (*Crassostrea gigas*) larval development: isotope shifts during early shell formation reveal sub-lethal energetic stress

Elizabeth L. Brunner[1,2], Fredrick G. Prahl[1], Burke Hales[1], George G. Waldbusser[1,*]

[1]College of Earth, Ocean, and Atmospheric Sciences, Oregon State University, Corvallis, OR 97331, USA

[2]*Present address:* Round River Conservation Studies, Salt Lake City, UT 84103, USA

ABSTRACT: Three cohorts of Pacific oyster (*Crassostrea gigas*) larvae at Whiskey Creek Shellfish Hatchery (WCH) in Netarts Bay, Oregon, were monitored for stable isotope incorporation and biochemical composition: one in May 2011 and two in August 2011. Along with measures of growth and calcification, we present measurements of stable isotopes of carbon in water, algal food, and the shell and tissue, and nitrogen in food and tissue across larval development and growth. These relatively unique measures through larval ontogeny allow us to document isotopic shifts associated with initiation and rate of feeding, and the catabolism of C-rich (lipid) and N-rich (protein) pools. Similar ontological patterns in growth and bulk composition among the cohorts reinforce prior results, suggesting that the creation of the initial shell is energetically expensive, that the major carbon source is ambient dissolved inorganic carbon, and that the major energetic source during this period is maternally derived egg lipids. The May cohort did not isotopically reflect its food source as rapidly as the August cohorts, indicating slower feeding and/or higher catabolism versus anabolism. Our measurements also document differences in bulk turnover of organic carbon and nitrogen pools within the larvae, showing far greater conservation of nitrogen than carbon. These stable isotope and bulk biochemical measurements appear to be more sensitive indicators of sub-lethal environmental stress than the commonly used metrics of development and growth.

KEY WORDS: Stable isotopes · Pacific oyster · Larvae · Ontology · Ocean acidification

INTRODUCTION

Bivalve larvae living in variable estuarine environments appear to be most sensitive to environmental stressors like low ambient calcium carbonate saturation state in the 2 d following fertilization, while they are forming the initial, or 'D-hinge', shell (Kurihara 2008, Barton et al. 2012, Gobler & Talmage 2013, Waldbusser et al. 2015a,b). Although the fundamental mechanism of this early sensitivity is of great interest (Waldbusser et al. 2013) and the subject of several recent reviews (regarding ocean acidification [OA]: Kroeker et al. 2010, 2013, Parker et al. 2013, Gazeau et al. 2013), there are several aspects of this early developmental stage that have not been fully explored. There have however been several studies of these early developmental stages in marine mollusks and bivalves (Labarbera 1974, Kniprath 1981, Mouëza et al. 2006), and it should be noted that the ability to develop to a fully shelled D-hinge larva has been used for decades as an eco-toxicological measure of environmental stress (e.g. His et al. 1997). One problem is how to adequately measure environmental stress effects that may carry over to later developmental stages. The effects of sub-lethal stress do not always manifest immediately, so popular growth and development metrics (e.g. length at D-hinge) cannot fully capture the physiological response. A 2012

*Corresponding author: waldbuss@coas.oregonstate.edu

study in a commercial Pacific oyster hatchery found that effects of early exposure to low saturation state water were not seen for more than a week (Barton et al. 2012). This 'carry over' effect was similar to those observed by (Hettinger et al. 2012, 2013) for *Ostrea lurida* and by Gobler & Talmage (2013) in *Mercenaria mercenaria*. Parental condition has also long been recognized as important for determining larval success (Gallager & Mann 1986, Gallager et al. 1986). Finally, many invertebrates have stage-based milestones for larval development, and stressed larvae tend to spend more time in the planktonic state (reviewed by Gazeau et al. 2013 with regards to OA). Slower growth can therefore be confused with failure to achieve developmental milestones. These all highlight the challenges in measuring responses of bivalve larvae to acidification stress using gross morphological features (Timmins-Schiffman et al. 2013).

To investigate the bioenergetic mechanism of stress in the early larval period, we followed 3 cohorts of Pacific oyster (*Crassostra gigas*) larvae through sublethal stress conditions at Whiskey Creek Shellfish Hatchery, in Netarts, Oregon. We measured the biochemical composition, growth, calcification, and energetic reserves of all 3 cohorts throughout the larval period, and also monitored the stable isotopes of the larval tissue and growing shell. These isotopic measurements, combined with measurements of the dissolved inorganic carbon (DIC) of their tanks and their algal food, allowed us to fully describe the movement of carbon and nitrogen into and out of the larvae. The measurements of stable C and N isotopes through larval development are novel, as far as we are aware, and help to further detail the energetic and developmental challenges faced by rapidly developing bivalve larvae. These non-traditional and comprehensive measurements are more sensitive to sub-lethal stress in larvae than commonly used metrics such as development benchmarks and growth.

During the vulnerable first 48 h, larvae secrete the Prodissoconch I (initial) shell (PDI), which involves different organs than Prodissoconch II shell formation and adult calcification. PDI shell biocalcification has not been described in nearly as much detail as later stages (see review in Kniprath 1981 for a general review on development at this stage). In particular, questions remain about the balance of shell carbon from metabolic and seawater DIC stages during PDI shell formation (Waldbusser et al. 2013). Larval oysters precipitate aragonite (a relatively soluble polymorph of calcium carbonate), which is a commonly cited rationale for predicting them to be losers in a high CO_2 world. However, thermodynamics cannot explain differential sensitivity within life-history stages with the same mineral polymorph (Waldbusser et al. 2010), nor sensitivity patterns found across taxa (Ries et al. 2009). Some studies suggest larval oyster shell is initiated as the unstable amorphous calcium carbonate (ACC) (e.g. Weiss et al. 2002, Mount et al. 2004), while others have found no evidence of ACC in the early larval shell (Kudo et al. 2010, Yokoo et al. 2011; and Medakovic 2000 notes amorphous tissue). Regardless of the polymorph, all bivalve larval shell is precipitated orders of magnitude more rapidly than precipitation would proceed abiotically in similarly supersaturated (with respect to calcium carbonate) seawater, and PDI shell is created fastest (Maeda-Martinez 1987, Waldbusser et al. 2013, 2016a,b). Bivalves employ 2 energy-demanding processes to overcome this kinetic constraint: the synthesis of organic matrix macromolecules that provides nucleation sites and catalyzes precipitation (Marin et al. 2008) and the alkalization of the calcifying fluid via proton pumping (McConnaughey & Gillikin 2008, Ries 2011). Previous estimates of these contributions highlight protein synthesis as a more energetically demanding process (Palmer 1992, Waldbusser et al. 2013). Recent work on sea urchin larvae confirms these findings, as a far greater increase in energetic expense under CO_2 stress is associated with protein synthesis than with cross-membrane ion transport (Pan et al. 2015).

Waldbusser et al. (2013) invoked a kinetic argument to explain how the energetic demand of the initial shell's precipitation increases exponentially as the ambient water calcium carbonate saturation state decreases but is not yet under-saturated. During the initial shell formation period, the larvae appear less able to exert biological control over the calcification process, and the high energetic demand required to complete the initial shell under lower calcium carbonate saturation conditions can result in a lower scope for growth, ultimately putting the larvae into an energetic deficit from which they do not appear able to recover (e.g. Barton et al. 2012). The equation used to describe this kinetic constraint is:

$$r = k(\Omega - 1)^n \quad (1)$$

where r is the mineral precipitation rate, k is the rate constant, Ω is the saturation state of the surrounding seawater with respect to the given mineral, and n is the reaction order constant.

We believe that this kinetic model describes the fundamental mechanism of larval bivalve sensitivity; however, it has 2 primary limitations. First, data from only 1 cohort of larvae were used. Second, it makes the assumption that the saturation state of the ambi-

ent seawater is equal to the saturation state of the calcifying space. We have acknowledged and addressed the second limitation elsewhere (Waldbusser et al. 2015a,b, 2016a,b). The present paper attempts to address the first limitation by validating the measurements from Waldbusser et al. (2013) with 2 additional cohorts of larvae under naturally variable carbonate chemistry conditions, and presents additional data on bulk biochemical characteristics over this developmental period.

MATERIALS AND METHODS

We sampled multiple commercial cohorts of Pacific oyster larvae, *Crassostrea gigas*, at the Whiskey Creek Shellfish Hatchery (WCH), Netarts, Oregon, USA, where carbonate chemistry within the hatchery is set by ambient Netarts Bay conditions, but food availability (ad libitum) and temperature (25°C) are controlled to optimal levels. The large (~400 million larvae) cohorts provided sufficient larvae to measure bulk biochemistry parameters, such as organic content and composition, while the sequential tank incubations allowed us to fully describe the possible isotopic sources incorporated into shell and tissue at discrete intervals during larval life (e.g. 0–2 d, 2–5 d).

Setting and experimental design

We followed 3 cohorts of approximately 400 million *Crassostrea gigas* larvae from fertilization through metamorphosis: 1 cohort in May 2011 and 2 in August 2011. WCH's spawning protocols are described in detail by Barton et al. (2012) and Waldbusser et al. (2013). Briefly, larvae are maintained in static 22 m^3 tanks, which have their water changed every 2–3 d, and they are fed daily (Table 1). The water for each tank change is pumped from Netarts Bay — a marine-dominated estuary on the northern Oregon coast (45.403°N, 123.944°W), which is flushed nearly every tidal cycle with water from the adjacent North Pacific Ocean (Whiting & McIntire 1985). With roughly two-thirds of the 9.41 km^2 aerial extent covered in *Zostera* spp. beds and the remaining tidal flats supporting microphytobenthos production, there is a diurnal PCO_2 (partial pressure of carbon dioxide) cycle that reflects the daily cycle of photosynthesis and respiration in spring and summer such that the highest PCO_2 values are seen in the morning after a night of respiration and the lowest PCO_2 values are seen in the afternoon (Waldbusser & Salisbury 2014). Thus, the saturation state at the hatchery intake pipe is variable on hourly, weekly, and seasonal timescales (Barton et al. 2012, Waldbusser & Salisbury 2014). To exaggerate the naturally occurring PCO_2 conditions of the upwelling season in August, water was pumped in the morning. May 2011 was a period of high freshwater input into Netarts Bay, and thus the water started with a lower salinity (~26) and lower alkalinity than usual (~1991 µmol kg^{-1}). For the May cohort, water for each tank-fill was pumped in the afternoon, when PCO_2 was relatively low. All water was heated to 25°C before being pumped into the tanks. The mean experimental tank temperature over the course of these experiments was 23.9°C, with a standard deviation of 1.71°C.

Spawn and larval culture

On 18 May 2011 and again on 14 August 2011 at least 3 Willapa Bay females were strip-spawned and fertilized with sperm from at least 1 Willapa Bay male. The fertilized eggs in August were split into 2

Table 1. Algal culture composition for May and August cohorts. Both cohorts of *Crassostrea gigas* in August received the exact same algal cultures in the same ratios and are therefore presented in this table combined. CISO: *Isochrysis* sp. (Caribbean); bbsCISO: CISO in bag system; TISO: *Isochrysis* sp. (Tahitian); NANO: *Nannochloropsis* sp.; CG: *Chaetoceros gracilis*; CCP: *Chaetoceros calcitrans*; 3H: *Thalassiosira pseudonana*; Blend: in-house mix of above taxa

Age	May	Aug
0	–	–
1	–	CISO
2	CSIO + CCP + bbsCISO	bbsCISO
3	bbsCISO	bbsCISO
4	bbsCISO	bbsCISO
5	bbsCISO	bbsCISO
6	bbsCISO	CISO
7	bbsCISO	CISO
8	bbsCISO	CISO + TISO
9	Blend + CISO	CISO
10	CISO	CISO + TISO
11	Blend + CISO	CISO + TISO
12	CSIO + CCP	bbsCISO
13	Blend	CISO + CCP
14	Blend + NANO + CCP	–
15	CISO + NANO + CCP	CG + CCP + CISO
16	CISO	CG + CISO
17	CISO + CCP	CG + CISO
18	TISO	CG + CISO
19		CG + CCP + CISO
20		CISO
21		CG + 3H

different tanks ~1 h after fertilization (a 'buffered' and a control tank, each starting with approximately 400 million larvae), and followed separately for the remainder of their larval period. The WCH buffer system treated incoming water with industrial grade soda ash (Na_2CO_3) to an aragonite saturation state (Ω_{ar}) equal to 4 during this experiment (Table 2, Fig. 1).

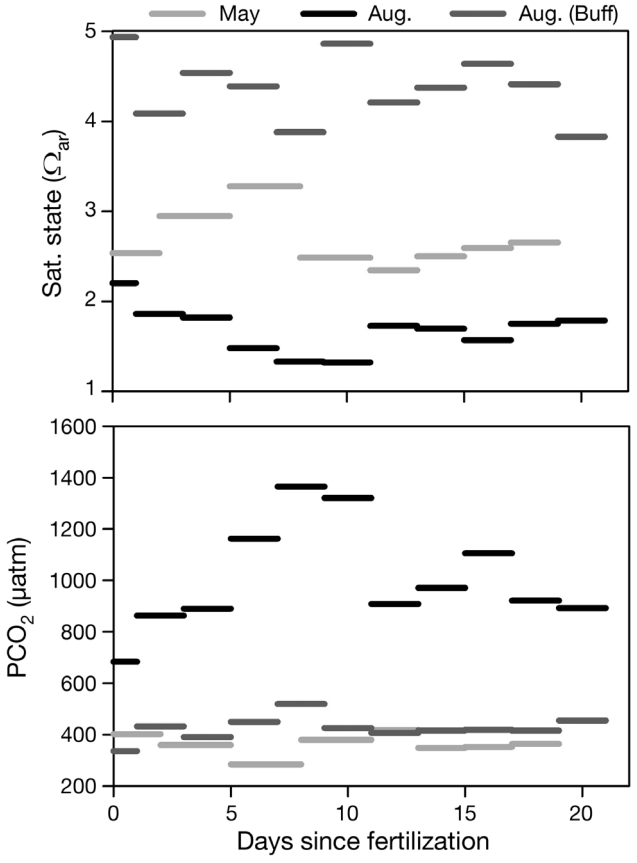

Fig. 1. Carbonate chemistry conditions (Ω_{ar} and PCO_2) for each tank incubation at Whiskey Creek Shellfish Hatchery, in Netarts Bay, Oregon. Water samples were taken as the tanks were filled, just prior to the addition of larvae or algae, and analyzed by standard methods at Oregon State University. Samples are represented as discontinuous bars to emphasize that the tanks were drained and re-filled with new Netarts Bay water at each tank change

All larvae were fed a rotating mixture of algal cultures grown at WCH, including *Isochrysis* sp., *Chaetoceros gracilis*, and *Chaetoceros calcitrans* (Table 1). In the first 5–10 d the larvae were fed *Isochrysis* sp. from a continuous culture bag system; these algae have a particularly low $\delta^{13}C$ signal (around −45‰) which is due to the bubbling of culture water with compressed industrial grade CO_2. At each feeding, between 200 and 800 ml of algal feed cultures were filtered onto pre-combusted 47mm GF/F glass fiber filters (Whatman), and the algae retained on the filter were dried at <45°C for storage until analysis. The sample volume was determined to account for different densities of algal culture and achieve optimal amounts of organic material on each filter for analysis.

At each tank water change, the previous tank's water was drained onto an appropriately sized sieve to capture all larvae, and the larvae were then transferred into a newly filled tank. A 0.5–2 g dry weight sub-sample (representing estimated 3–10 × 10^6 2-d-old larvae or 2–9 × 10^5 19-d-old larvae) of the cohort was collected from the sieve, briefly rinsed with DI water, and immediately frozen. The samples were then freeze-dried within 3 wk of collection (Labconco FreeZone 6 Freeze Drier). As all the larvae from each cohort were living in the same tank, taking multiple primary samples would have been pseudo-replication; we therefore assume that the sub-samples accurately represent the entire larval cohort. In May, after 5 d, the fastest growing larvae were selected by passing the cohort through an 80 µm sieve, which caught about half of the larvae. This procedure for poorly performing cohorts is commonly employed at WCH. The August cohorts were not sorted via this size-fraction screening as their general growth and fitness were better.

Isotopic and compositional measurements of larvae and algae

All stable carbon isotope samples were analyzed in Oregon State University's College of Earth, Ocean,

Table 2. Means (±SD) of carbonate chemistry from tank incubations for each cohort of *Crassostrea gigas*. Tanks were heated to ~25°C prior to each tank filling, and rarely cooled to <23°C between tank fillings. PCO_2: partial pressure of carbon dioxide; DIC: dissolved inorganic carbon; Talk: total alkalinity; pH_{sws}: pH (seawater scale) ; Ω_{ar}: argonite saturation state; buff: buffered

	Salinity (psu)	PCO_2 (µatm)	Talk (µmol kg^{-1})	DIC (µmol kg^{-1})	pH_{sws}	Ω_{ar} mean	Ω_{ar} at spawn
May (n = 8)	26.6 ± 2.3	364 ± 40	1991 ± 78	1758 ± 50	8.04 ± 0.04	2.6 ± 0.3	2.4
Aug (n = 11)	32.7 ± 0.6	1008 ± 207	2318 ± 151	2181 ± 68	7.71 ± 0.16	1.6 ± 0.2	2.1
Aug (buff) (n = 11)	32.8 ± 0.6	425 ± 45	2842 ± 91	2452 ± 81	8.09 ± 0.04	4.2 ± 0.3	4.6

and Atmospheric Sciences Stable Isotope Laboratory. Detailed descriptions of these standard protocols can be found in Waldbusser et al. (2013) and at stableisotope.coas.oregonstate.edu/. All runs were calibrated and checked with NIST-certified and in-house-calibrated standards. Precision and accuracy are noted for each analysis.

To measure larval tissue $\delta^{13}C$ and $\delta^{15}N$, 6–10 mg freeze-dried larvae in Ag boats were acidified in a concentrated HCl atmosphere following the method of Hedges & Stern (1984). The samples were dried overnight, encapsulated in Sn boats, and loaded into a Costech Zero Blank Autosampler. Samples were flash combusted at >1020°C using a Carlo Erba NA1500 Elemental Analyzer (Verardo et al. 1990), and the resulting gas was analyzed by continuous-flow mass spectrometry using a DeltaPlus XL isotope ratio mass spectrometer. Hole punches of filter (diameter ~7 mm) with dried algae were analyzed via the same method as the larval tissue, without the acidification step. Repeatability of samples was 0.21‰ for $\delta^{13}C$ and 0.27‰ for $\delta^{15}N$.

In order to measure larval shell carbonate $\delta^{13}C$, we reacted 19–50 freeze-dried larvae with concentrated phosphoric acid at 70°C for 5 min in a Finnigan Keil III device. The resulting CO_2 was isolated from other reaction products and measured on a MAT 252 mass spectrometer by dual inlet mass spectrometry. Accuracy was better than ±0.05‰, and repeatability was ±0.02‰.

Elemental analysis (CHN) of decalcified larvae provided an independent check of the lipid proportion. Assuming that the 3 major bulk biochemical components of larval mass are carbohydrate, lipid, and protein, and that carbohydrate is a minor constituent (e.g. His & Maurer 1988, Moran & Manahan 2004), an elevated C:N ratio indicates a greater lipid:protein ratio. Larval samples were analyzed for organic and inorganic elemental composition before and after acidification as described above on a Carlo Erba NA-1500 elemental analyzer calibrated with at least 6 acetanilide standards following the methods of Verardo et al. (1990). Ash-free dry weight (AFDW) was determined by weight comparison before and after combustion at 490°C for 4 h.

Extractable lipids, length, and SEM imaging

At each tank change, an aliquot of larvae was fixed in 2.5% gluteraldehyde and 1% paraformaldehyde in a 0.1 M cacodylate buffer. Samples were later transferred to 50% ethanol and imaged using an Olympus SZH10 dissecting microscope attached to a Fuji S20 digital SLR with 6.1 M pixels. Shell length (longest axis parallel to hinge) was measured on 100 larvae per sampling point (ImageJ 1.44p). Shell lengths were converted into weights using the dry-tissue weight to length relationship for larval *Crassostra gigas* from Bochenek et al. (2001).

To measure extractable lipids, ~75 mg samples of freeze-dried larvae were extracted on a Dionex ASE 200 accelerated solvent extractor for 4 cycles of 5 min at 1500 psi with 3:1 methylene chloride:methanol. The extracts were combined with 25 ml hexane and washed against 10 ml 50% saturated NaCl to remove hydrophilic impurities (proteins, carbohydrates). The aqueous phase was drained away, and the lipid-containing fraction was dried under an N_2 gas stream. The lipid concentrate was then re-suspended in 500 µl CS_2 and an aliquot (100 µl) moved to a tared nickel weighing boat, dried, and re-weighed to obtain the gravimetric weight of lipid. This weight was compared to the original sample weight to determine the fraction of total lipid. As with the other bulk measurements, these values were normalized to larval weights to estimate lipid (ng) per larvae. Additionally, it should be noted that the lipid measurements by Waldbusser et al. (2013) may be an over-estimate, due to the gravimetric extraction method used. The washed values presented here provide a better estimate of the true lipid content. Due to a sampling error, we do not have a reliable washed lipid value for the 48 h time point for the May cohort. Given the similarity between the washed and unwashed values in early life, we used the unwashed gravimetric lipid weight (as reported in Waldbusser et al. 2013) instead.

Carbonate chemistry

Water samples were collected at each tank filling prior to the addition of larvae or algae. For DIC ^{13}C analysis, aliquots of $HgCl_2$-fixed sample were pipetted into Labco glass vials and sealed with rubber septa caps. The vials were cooled to 13°C, allowed to equilibrate for 15 min, and purged with He for 5 min each. Phosphoric acid (85%) was then added to each vial via syringe. The samples were left to equilibrate for 10 h and analyzed via continuous-flow mass spectrometry using a GasBench-DeltaV system. Each run was standardized using a combination of sodium bicarbonate (3 mM in solution) and calcium carbon-

ate standards. These methods have a precision of 0.15‰ and a repeatability better than 0.2‰.

Samples for PCO_2 and DIC analysis were collected at each water change in 330 ml amber glass bottles, poisoned with $HgCl_2$, and analyzed following Bandstra et al. (2006) The uncertainty of these measurements is <2% and 0.2% for PCO_2 and DIC, respectively. The remaining carbonate system parameters were calculated using the carbonic acid dissociation constants of Millero (2010), the boric acid constants as defined by Dickson (1990), and the aragonite solubility as defined by Mucci (1983).

Statistical analyses and isotope calculations

In these cohorts, the stable isotopic composition of shell, larval tissues, and food were used as tracers of carbon and nitrogen sources during larval shell formation and development. Stable nitrogen and carbon isotopic data provide independent estimates of the rate of incorporation of exogenous food into larval tissue. The estimate is a function of the feeding rate (gain) and the catabolism of energy stores (loss). Thus, a simple mass-balance of organic carbon (OC) and nitrogen (ON) was constructed. Isotope values of the tissue at each time point and the algal diet were used to constrain the model and to calculate a mass loss (e.g. respiration, excretion) and a mass gain (e.g. assimilation) of both OC and ON during each tank change until the tissue began to overlap with the algal signal.

The fraction metabolic carbon in the shell at each time-point was calculated using the method of McConnaughey et al. (1997) using the inputs of tissue $\delta^{13}C$ to approximate the respired carbon in the calcifying fluid, the $\delta^{13}C$ of the ambient DIC during the most recent tank change, and the $\delta^{13}C$ of the larval shell. The abiotic equilibrium fractionation between aragonite and bicarbonate (Δ) was taken from Romanek et al. (1992).

$$R(\delta^{13}C_{resp}) + (1-R)(\delta^{13}C_{DIC}) = \delta^{13}C_{shell} - \Delta \quad (2)$$

where R is the proportion of metabolic contribution to shell, $\delta^{13}C_{resp}$ is the isotope value of respired carbon approximated from larval organic tissue, $\delta^{13}C_{DIC}$ is the isotope value of the ambient DIC, $\delta^{13}C_{shell}$ is the isotope value of the shell, and Δ is the abiotic fractionation factor between aragonite and bicarbonate (Romanek et al. 1992).

All statistical analyses were done in the statistical program 'R' (2.15.2), and used the package 'multcomp'.

RESULTS

Carbonate chemistry

Mean carbonate chemistry conditions in May were characterized by near-atmospheric PCO_2 and a moderate Ω_{ar} (2.6), while upwelling in August generated a higher mean PCO_2 and lower mean Ω_{ar} (1.6). (Fig. 1, Table 2). In general, the August unbuffered cohort saw high PCO_2 water with a correspondingly low saturation state, although upwelling intensity varied over the 21 d period and was strongest between 5 and 10 d post-fertilization. The August buffered cohort experienced the same upwelled water, but the water was buffered by the addition of Na_2CO_3 to decrease the PCO_2 and increase $\Omega_{ar.,}$ These compositional differences can be seen in respective values of PCO_2 and Ω_{ar}. A 1-way ANOVA showed significantly different mean Ω_{ar} among cohorts, $F_{(2,27)} = 219$, $p \leq 0.0001$, and a post hoc Tukey comparison of the 3 groups indicated that all comparisons were significant when $\alpha = 0.05$. The lowest mean tank saturation state was seen in the August unbuffered tanks, while the highest was seen in the buffered tanks, with the May tanks having an intermediate mean saturation state. On average, the change in saturation state over each tank change was <0.3. The largest change in saturation state over the course of a single tank incubation occurred in the August unbuffered cohort during the 5th tank incubation (0.55 change in Ω_{ar}, accompanying a ~660 µatm decrease in PCO_2).

Calcification, growth, and bulk biochemistry

Mean shell length (a proxy for growth) was similar among all 3 cohorts, while soft tissue proxies such as AFDW, lipid bulk, and C:N ratio of tissue were more variable (Fig. 2, Table 3). In all cohorts, the lipids were drawn down rapidly during the first 2–5 d, reaching a low 5–10 d after fertilization. Maximum per larva lipid stores were seen 19 d after fertilization for all cohorts. This time point was our last sample period for the May cohort and 1 sample period before the end of the study for the August cohorts. We ended the study when most of the cohort reached the settlement size metric used at Whiskey Creek Hatchery.

The lipid fraction of the AFDW was similar for the 2 August cohorts, which came from the same broodstock. In contrast, the May cohort, despite having a higher lipid fraction than the 2 August cohorts, had a lower per larva lipid mass, the result of the May cohort's relatively low AFDW and slightly smaller

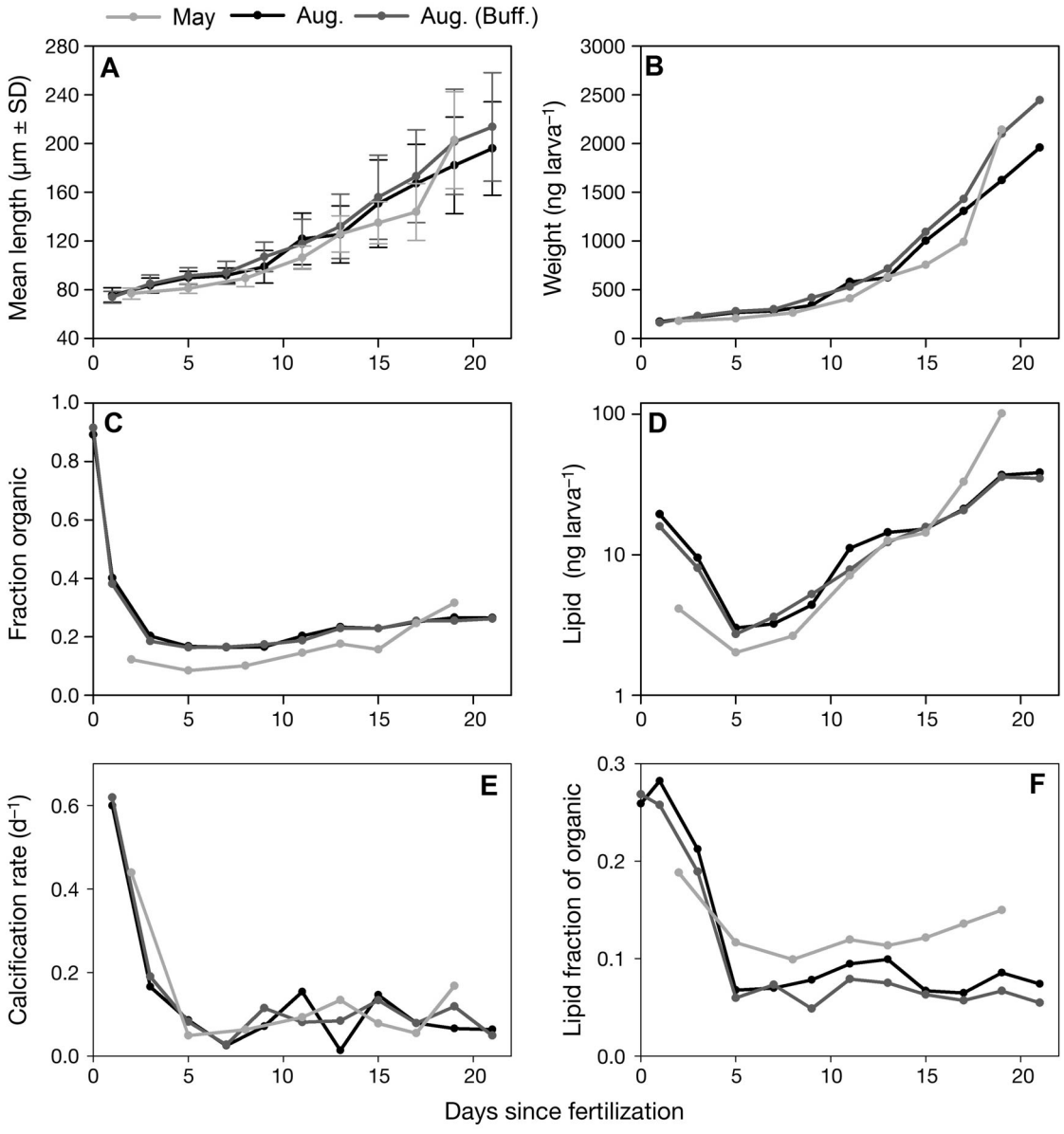

Fig. 2. Biochemical measurements of *Crassostrea gigas* larvae at each tank change. (A) Mean length of larvae (±SD). (B) Dry weight per larva, calculated using the length to dry weight relationship from Bochenek et al. (2001). (C) Fraction organic material (ash-free dry weight; AFDW). (D) Calculated lipid mass per larva. (E) Mass-normalized calcification rate. (F) Lipid fraction of AFDW (organic material)

mean weight. During PDI formation (0–2 d), all cohorts had a relatively high mean C:N atomic ratio of around 5.6, and this ratio decreased with age until ~10 d, after which point C:N values in the May cohort started to increase while both August cohorts showed a decrease. Note that total organic content was higher in the August cohort (Fig. 2).

Calcification rates were similar among all cohorts. The highest rates (~0.6 d^{-1}) were seen during the formation of the initial shell (0–1 d) and decreased rapidly to reach a near-constant rate (~0.1 d^{-1}) between 5 and 21 d after fertilization.

Stable isotopes

Stable isotope values over time are shown in Fig. 3. All cohorts showed decreasing shell $\delta^{13}C$ and an increasing metabolic carbon contribution with time, but there were differences among the cohorts in their

Table 3. Size, weight, and bulk biochemical measurements of Pacific oyster larvae through development and across the 3 different cohorts noted. Units are noted in each column header, and composition values of C and N are in proportions

Days	Fract. lipid (wt/wt)	Fract. organic (AFDW)	Length (µm) Mean ± SD	Weight (ng larva^{-1})	Lipid (ng larva^{-1})	Total N (wt/wt)	Total C (wt/wt)	Organic N (wt/wt)	Organic C (wt/wt)	Tissue atomic C:N	Calcif. rate (d^{-1})
Aug cohort											
0	0.231	0.89	–	–	–	–	–	–	–	–	–
1	0.113	0.40	76 ± 6	172	19	0.05	0.27	0.04	0.18	5.7	0.60
3	0.043	0.20	83 ± 6	221	10	0.02	0.19	0.02	0.08	5.2	0.17
5	0.011	0.17	90 ± 5	266	3	0.02	0.17	0.02	0.07	5.1	0.09
7	0.011	0.16	92 ± 6	282	3	0.02	0.17	0.02	0.07	4.8	0.02
9	0.013	0.17	99 ± 13	341	4	0.02	0.18	0.02	0.08	4.9	0.07
11	0.019	0.20	122 ± 21	581	11	0.02	0.19	0.02	0.08	5.0	0.15
13	0.023	0.23	125 ± 23	625	14	0.03	0.20	0.03	0.11	4.8	0.01
15	0.015	0.23	151 ± 36	1001	15	0.03	0.20	0.03	0.10	4.5	0.15
17	0.016	0.25	167 ± 32	1306	21	0.03	0.21	0.03	0.11	4.6	0.08
19	0.023	0.27	182 ± 40	1624	37	0.03	0.21	0.03	0.12	4.7	0.07
21	0.020	0.26	196 ± 38	1959	38	0.03	0.21	0.03	0.12	4.4	0.06
Aug (buff) cohort											
0	0.246	0.92	–	–	–	0.09	0.49	–	–	–	–
1	0.098	0.38	74 ± 5	162	16	0.04	0.27	0.04	0.17	5.5	0.62
3	0.035	0.18	85 ± 7	231	8	0.02	0.18	0.02	0.08	4.7	0.19
5	0.010	0.16	91 ± 7	279	3	0.02	0.17	0.02	0.07	4.8	0.08
7	0.012	0.16	94 ± 9	299	4	0.02	0.20	0.02	0.07	4.5	0.03
9	0.008	0.17	107 ± 12	418	5	0.02	0.18	0.02	0.07	4.5	0.11
11	0.015	0.19	118 ± 20	530	8	0.02	0.18	0.02	0.08	4.7	0.08
13	0.017	0.23	132 ± 26	715	12	0.03	0.20	0.02	0.10	4.8	0.08
15	0.014	0.23	156 ± 35	1093	16	0.03	0.20	0.03	0.10	4.6	0.13
17	0.014	0.25	173 ± 38	1430	21	0.03	0.20	0.03	0.11	4.6	0.08
19	0.017	0.25	201 ± 43	2102	36	0.03	0.21	0.03	0.11	4.5	0.12
21	0.014	0.26	214 ± 45	2445	35	0.03	0.21	0.03	0.12	4.4	0.05
May cohort											
2	0.023	0.12	77 ± 5	179	4	0.01	0.16	0.01	0.05	5.8	0.44
5	0.010	0.08	81 ± 4	205	2	0.01	0.14	0.01	0.03	4.8	0.05
8	0.010	0.10	89 ± 7	264	3	0.01	0.15	0.01	0.04	4.5	0.06
11	0.017	0.14	106 ± 10	411	7	0.02	0.17	0.02	0.06	4.4	0.09
13	0.020	0.18	126 ± 15	631	13	0.02	0.18	0.02	0.08	4.9	0.13
15	0.019	0.16	135 ± 17	756	14	0.02	0.18	0.02	0.07	4.9	0.08
17	0.033	0.25	144 ± 23	990	33	0.03	0.21	0.02	0.10	4.9	0.05
19	0.047	0.32	203 ± 40	2142	101	0.04	0.24	0.03	0.15	5.7	0.17

estimated incorporation of metabolic carbon (Fig. 4, Table 4).

DISCUSSION

This study was designed to be an experimental comparison among groups of larval oysters, rather a comprehensive study of the stable isotope composition and related biochemical changes of larvae, and we were able to do this on 3 cohorts (1 of which was similar in parents but subjected to different conditions in the hatchery). This approach was required given the numbers of larvae needed, particularly at the smallest stages, to provide reliable measurements of the stable isotopes and biochemical composition. We therefore highlight the patterns and notable observations from these 3 different cohorts of larvae, and encourage others to verify these findings in different studies. Three general observations are notable and supported by the data from this study: (1) the elevated energetic demands during the development to PDI are evident among groups, although subtle differences exist; (2) in general the biochemical condition and growth data showed little difference among cohorts, and, in all 3 cohorts, PDI development occurred in generally favorable chemistry; and (3) the stable isotopes appeared to be more sensitive to differences among the cohorts than most of the more broadly used measures of stress effects.

The carbonate chemistry conditions for all cohorts were variable, but within the range of previous observations in Netarts Bay, Oregon (Barton et al. 2012), and the carbonate chemistry conditions were favorable ($\Omega_{ar} > 1.6$) at the time of spawning for generally good development to swimming veligers. Accordingly, none of the 3 cohorts differed significantly in the standard metrics used for growth or development in typical ocean acidification experiments.

The May cohort, however, had a lower AFDW than either of the August cohorts throughout most of the study period. This pattern differs from the typical

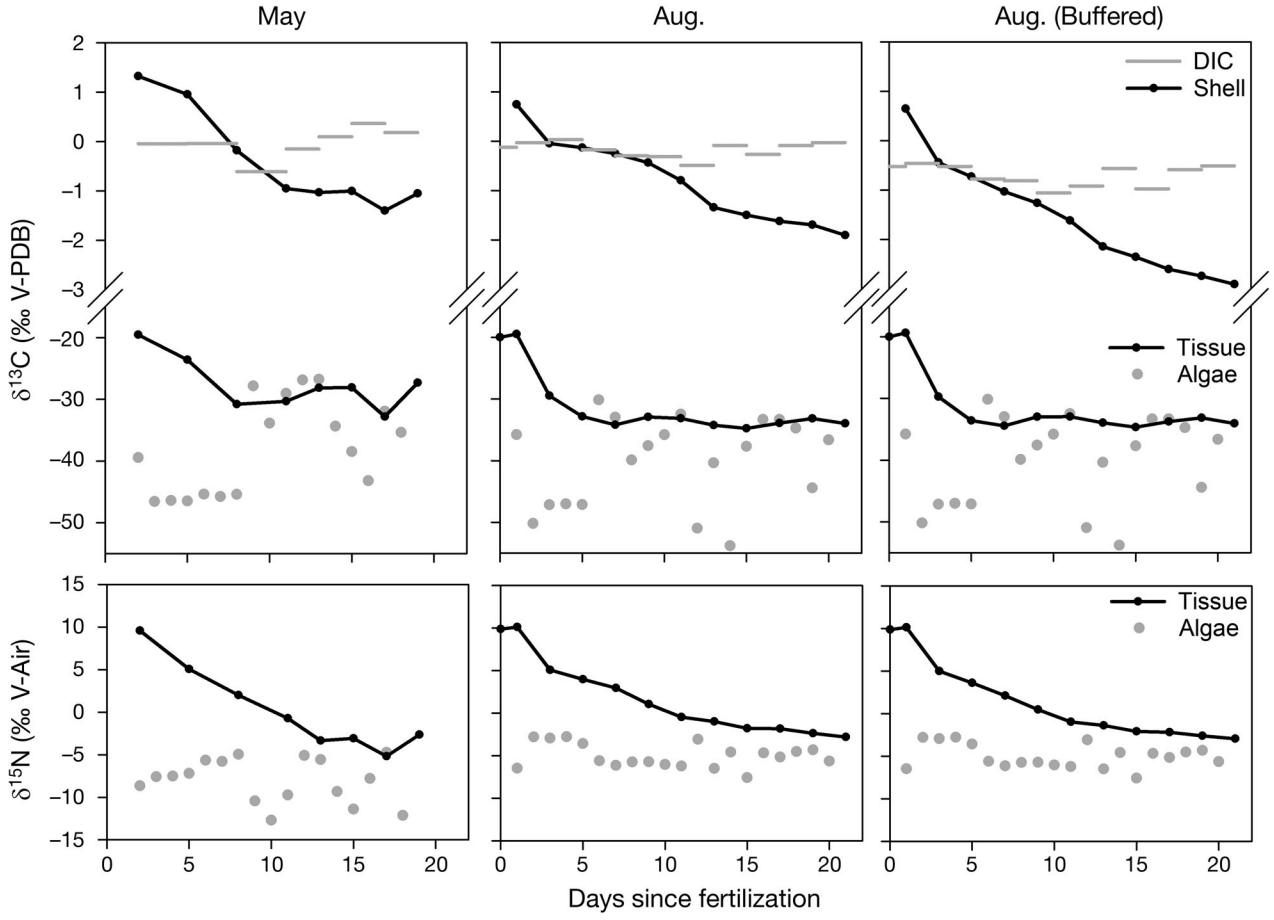

Fig. 3. Stable isotopes ($\delta^{13}C$, $\delta^{15}N$) of tissue and shell of *Crassostrea gigas*, ambient dissolved inorganic carbon (DIC) and algae. Top panels show stable isotopes of carbon ($\delta^{13}C$, in ‰ V-PDB) in tank DIC (gray bars), larval shell (black line above break), larval tissue (black line below break), and algae (gray circles below break). Bottom panels show stable isotopes of nitrogen ($\delta^{15}N$, in ‰ V-Air) in larval tissue (black line) and algae (gray circles)

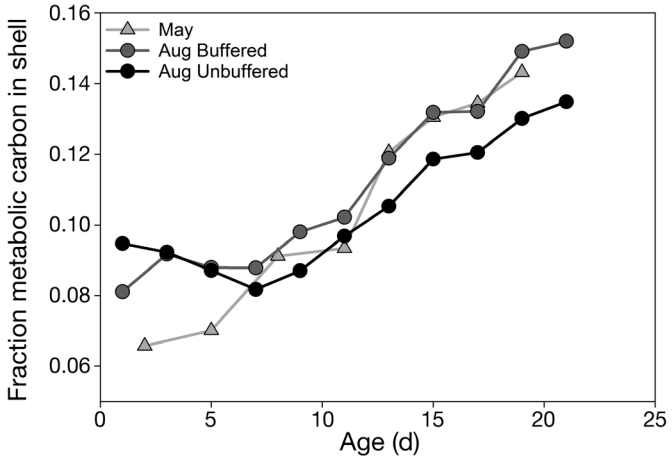

Fig. 4. Calculated fraction metabolic carbon in shell DIC for all 3 cohorts of *Crassostrea gigas*, based on isotope mixing model. Importantly the slight differences in DIC $\delta^{13}C$ due to buffering are accounted for in the model and are not responsible for the differences between the August cohorts

suite of observed responses to acidification (e.g. Barton et al. 2012) and, therefore, provides unique insight into potential mechanisms of resiliency. In particular, our data highlight the role of maternal lipids in helping larvae deal with unexpected energetic expenses, such as the creation of the initial shell, under less favorable carbonate chemistry conditions. The May cohort began with lower lipid content than the August cohorts, likely due to differences in broodstock conditioning. So while the unbuffered August cohort was living under moderate acidification stress caused by upwelling — which is expected to increase energetic demand — they also had more lipid reserves from which to draw.

Well known key factors influencing larval success include: food availability, environmental conditions, and egg lipid content or other 'maternal effects' (Gallager & Mann 1986, Kennedy 1996, Bochenek et al. 2001). In general, egg quality is associated with egg

Table 4. Stable isotopes of carbon ($\delta^{13}C$ V-PDB) and nitrogen ($\delta^{15}N$) from tissue, shell, and diet of all 3 cohorts of *Crassostrea gigas*. All analyses were completed in the CEOAS Stable Isotope Laboratory following standard analytical protocols. Both cohorts in August received the exact same algal cultures in the same ratios and are therefore presented in this table combined. DIC: dissolved inorganic carbon; buff: buffered

Days since fertilization	Tissue $\delta^{13}C$			Tissue $\delta^{15}N$			Algal $\delta^{13}C$		Algal $\delta^{15}N$		Shell $\delta^{13}C$			DIC $\delta^{13}C$		
	May	Aug	Aug (buff)	May	Aug	Aug (buff)	May	Aug	May	Aug	May	Aug	Aug (buff)	May	Aug	Aug (buff)
0	–	−20.00	−20.00	–	9.87	9.87	–	–	–	–	–	–	–	–	−0.12	−0.52
1	–	−19.48	−19.38	–	10.10	10.12	–	−35.77	–	−6.48	–	0.75	0.65	–	−0.03	−0.46
2	−19.55	–	–	9.58	–	–	−39.47	−50.19	−8.66	−2.81	1.33	–	–	−0.04	–	–
3	–	−29.46	−29.73	–	5.07	4.98	−46.58	−47.15	−7.60	−2.96	–	−0.04	−0.44	–	0.03	−0.52
4	–	–	–	–	–	–	−46.42	−47.01	−7.52	−2.79	–	–	–	–	–	–
5	−23.60	−32.84	−33.57	5.05	3.97	3.62	−46.49	−47.13	−7.21	−3.59	0.96	−0.13	−0.72	−0.04	−0.17	−0.77
6	–	–	–	–	–	–	−45.38	−30.16	−5.67	−5.60	–	–	–	–	–	–
7	–	−34.17	−34.44	–	2.94	2.11	−45.79	−32.97	−5.82	−6.15	–	−0.25	−1.03	–	−0.29	−0.81
8	−30.80	–	–	2.00	–	–	−45.42	−39.91	−4.96	−5.75	−0.18	–	–	−0.61	–	–
9	–	−32.92	−32.96	–	1.05	0.47	−27.85	−37.57	−10.44	−5.74	–	−0.43	−1.26	–	−0.31	−1.06
10	–	–	–	–	–	–	−33.89	−35.82	−12.71	−6.04	–	–	–	–	–	–
11	−30.32	−33.15	−32.95	−0.73	−0.47	−0.96	−29.04	−32.48	−9.74	−6.24	−0.95	−0.79	−1.61	−0.15	−0.49	−0.92
12	–	–	–	–	–	–	−26.89	−50.96	−5.11	−3.09	–	–	–	–	–	–
13	−28.14	−34.23	−33.94	−3.34	−0.99	−1.38	−26.76	−40.37	−5.60	−6.50	−1.03	−1.34	−2.14	0.10	−0.08	−0.56
14	–	–	–	–	–	–	−34.38	−53.80	−9.35	−4.59	–	–	–	–	–	–
15	−28.10	−34.76	−34.66	−3.09	−1.79	−2.08	−38.49	−37.70	−11.41	−7.59	−1.00	−1.50	−2.35	0.37	−0.27	−0.97
16	–	–	–	–	–	–	−43.19	−33.32	−7.81	−4.69	–	–	–	–	–	–
17	−32.95	−33.90	−33.74	−5.18	−1.83	−2.19	−31.95	−33.32	−4.75	−5.17	−1.40	−1.62	−2.60	0.18	−0.09	−0.58
18	–	–	–	−4.92	–	–	−35.38	−34.73	−12.15	−4.52	–	–	–	–	–	–
19	−27.31	−33.18	−33.14	−2.64	−2.37	−2.61	–	−44.41	–	−4.32	−1.05	−1.69	−2.74	–	−0.02	−0.51
20	–	–	–	–	–	–	–	−36.64	–	−5.64	–	–	–	–	–	–
21	–	−33.97	−34.04	–	−2.81	−2.94	–	–	–	–	–	−1.90	−2.91	–	–	–

size; however, these two are not always correlated (see discussion in Moran & McAlister 2009 and references therein). Egg quality further varies both seasonally and in response to conditioning (Muranaka & Lannan 1984, Gallager & Mann 1986). Eggs from the August cohort had a lipid fraction of AFDW of ~26%, which is at the high end of reported literature values (Gallager et al. 1986, Massapina et al. 1999, Uriarte et al. 2004). The lipid fraction of the May cohort was not measured, but, given the low lipid stores in early larval life (at 48 h compared to the August cohorts), the total lipid content was likely to have been near the low end of literature values. The estimated per-larva lipid mass for the May cohort 5 d after fertilization (~2 ng larva^{-1}) would be expected from their structural lipids alone (Moran & Manahan 2004), which suggests that the larvae had used up all their energy stores by this point. This situation could be due to a low starting egg lipid content as mentioned above, which can limit larval growth and survival (Gallager & Mann 1986, Bochenek et al. 2001). Another potential factor influencing the cohorts was salinity variation between tank changes. *Crassostra gigas* larvae are hardy over a range of salinity conditions spanning those seen in May (23.8–30.1) (e.g. His et al. 1989, Bochenek et al. 2001). However, the May cohort experienced an environmentally unlikely instantaneous change in salinity between tank changes from 29.7 to 24.9 at 8 d, which likely altered their energetic budget at later larval stages due to osmotic stress (McFarland et al. 2013).

Our data also underscore the sensitivity of the larvae to ambient conditions during the first 24 h of development. Growth of the non-buffered and buffered (August) cohorts was similar; however, spawning conditions for both cohorts were above Ω_{ar} = 2 (Fig. 1). Variation in carbonate chemistry conditions after this period did not necessarily alter physiological metrics such as growth and biochemical measures of energetic reserves. Waldbusser et al.

(2013) proposed that acidification-caused energetic stress in early larval life is likely caused by higher energy expenditure on initial shell formation via a kinetic barrier imposed by the developmental requirement for rapid shell calcification (Waldbusser et al. 2013, 2016a,b). As expected, the highest rates of shell calcification were found during the formation of the initial shell (Fig. 2E), confirming the experimental results of Maeda-Martinez (1987). These early formation rates are very conservative estimates given more recent documentation of early shell development (Waldbusser et al. 2015a, 2016b). Calcification rates decreased as a function of age as described elsewhere (Maeda-Martinez 1987, Waldbusser et al. 2013). PDI formation occurs rapidly between 13 and 16 h in *C. gigas* (Waldbusser et al. 2015a), and is structurally and compositionally distinct from later shell (Waller 1981, Yokoo et al. 2011). Our estimates reported here are, however, averages over a 2 d period; direct measures of the calcification rate during PDI formation are much faster than those reported here (Waldbusser et al. unpubl. data).

Starvation experiments with bivalve larvae have shown that without exogenous food inputs, survival (but not growth) is possible far beyond the calculated exhaustion of maternally derived energy, and dissolved organic matter (DOM) is the most frequently suggested alternate food source for larvae under such starvation conditions (Moran & Manahan 2004, Tang et al. 2006, Matias et al. 2011). It is critical to note that assimilation of DOM by oyster larvae appears to support only survival and not growth (Moran & Manahan 2004), and it has not been documented whether larvae starved for extended periods of time can successfully metamorphose. Additionally, the mantle tissue has been identified as the organ responsible for DOM uptake (Widdows 1991); the pre-cursor for the mantle does not develop until completion of the PDI shell. Thus, during the most energetically demanding calcification stage, it is unclear whether developing embryos would have access to supplemental energy through direct DOM uptake. We have, therefore, made the assumption that the early larvae act as a 'closed' metabolic system (e.g. Bochenek et al. 2001, Emmery et al. 2011). If the early larvae were assimilating DOM, it could bias our model results. Estimates of the $\delta^{13}C$ and $\delta^{15}N$ of DOM in the open Pacific and/or California Current System range from −21 to −23‰ for $\delta^{13}C$ and 6.7 to 9.7‰ for $\delta^{15}N$ (Benner et al. 1997, Bauer et al. 1998, Walker & McCarthy 2012) — closer to our 'maternal' egg signal than to the food source. Therefore, any bias created by the incorporation of DOM would overestimate the contribution of maternal lipid to the total larval energy budget, again only subsidizing the respiratory component of the energy budget, not growth and development.

Total organic and lipid content in early life decreased dramatically during embryogenesis, as larvae catabolized maternally derived lipids and precipitated inorganic shell. At approximately 5 d post-fertilization, there was a 'low' in larval tissue content and lipid stores; a similar pattern in lipid concentrations was seen by His & Maurer (1988) in a wild population of *C. gigas*. The timing of this compositional minimum also corresponds to the 'lazy-larvae' syndrome that was noted in the Whiskey Creek Shellfish Hatchery — viable fully fed larvae that sink to the bottom of culture tanks and do not seem to recover. Following exposure to lower Ω_{ar} during initial shell formation, larvae would terminate swimming and sink to the bottom of the culture tanks several days later. While the larvae would remain viable, they would, in general, stop growing, and the cultures would be abandoned by the hatchery. It seems very likely that less maternal egg lipids or stress resulting in greater energy utilization during PDI shell formation results in an energetic low from which the larvae may not be able to recover. These patterns of OA induced carry-over effects were documented by Barton et al. (2012), but are also reflective of general carry-over effects found in other benthic invertebrate species subjected to other stressors (Pechenik 2006, Hettinger et al. 2013). There was also a slight decrease in lipid accumulation, growth rates, and AFDW between 10 and 15 d for all cohorts (Fig. 2). This period occurs after the end of the calculated maternal energy stores (Waldbusser et al. 2013) and is perhaps analogous to the trend of decreased survivorship between 14 and 19 d that was noted by Matias et al. (2011) in the clam *Ruditapes decussatus*; this trend was attributed to the decreased feeding and increased biochemical demands associated with the preparation for metamorphosis to adult benthic stages. Maximum per larva lipid stores were seen 19 d after fertilization for all cohorts, as expected when preparing for metamorphosis

The larval tissue isotope values can be thought of as a weighted average of all of the carbon that (1) begins in the eggs, (2) has entered the tissue pool from algae consumed, or (3) leaves the system as metabolic carbon dioxide or excreted nitrogen. The variability in algal isotopes comes from differences in algal species (Table 1) and the quantity of industrial tanked CO_2 that was bubbled into each algal culture, which generally has a much lighter $\delta^{13}C$ than seawater DIC (see Maberly et al. 1992, Rau et al. 1996,

Raven et al. 2002 for more info on C isotope fractionation in marine plants). For example, the periods of time with similar isotope values (i.e. 2–5 d for the August cohorts) all came from the same continuous bag culture system. The initiation of feeding is reflected in the rapid decrease in $\delta^{13}C$ as the tissue of the larvae starts to reflect the more depleted exogenous food source, which is most notable in the August cohorts, where the earliest samples were taken more frequently than in May. Indeed, the August cohorts were sampled at fertilization and when they were 1 d old, and the embryogenesis period generally occurs between these time points, as the larvae have not yet begun to feed. The larvae show decreasing C and N isotopic ratios for about 7 d, when they stabilize around a value that is 2–3‰ heavier than the average of their algal food, indicating that they have used up most of the maternal (heavier) stores of carbon (lipids) and nitrogen (proteins). The stable isotope data also indicate that the larvae reflected the carbon signal of their food source more rapidly than they did the nitrogen signal (Fig. 3), indicating rapid catabolization of lipids in early life, with organic carbon pools turning over more rapidly than those of organic nitrogen. This inference is corroborated by the corresponding decrease in AFDW, percentage lipid contribution to total mass, and C:N ratio of their tissue (as noted above). These conserved developmental patterns in lipid catabolism, bulk composition, and calcification rate among cohorts suggest that the creation of the initial shell is energetically expensive and that the major energetic source during this period is maternally derived egg lipids (Waldbusser et al. 2013). The evidence also suggests that there is little phenotypic plasticity at this critical developmental stage, which, if possible, could permit changes in calcification rate, thus alleviating the kinetic barrier.

The observed decreasing shell $\delta^{13}C$ with time could indicate either an increasing fraction of metabolic carbon in the shell or that the metabolic carbon being incorporated is becoming lighter (as the tissue from which it is derived approaches the lighter algal food source). These effects were disentangled using a 2 end-member mixing model (McConnaughey et al. 1997), which recorded generally increasing incorporation of $\delta^{13}C$-depleted metabolic carbon into larval shell with age (with subtle differences discussed below), indicating greater reliance on ambient DIC during the formation of the PDI shell and suggesting a mechanism of greater vulnerability (greater exposure) to the speciation of ambient DIC during this period. The ontogenic changes in stable carbon and nitrogen isotope composition observed here have not been well documented before in bivalve larvae, other than by Waldbusser et al. (2013), who presented data only from the May cohort. Our present $\delta^{13}C$ values for the shell of late-stage Pacific oyster larvae do match well with those of Owen et al. (2008) for 17 d old Atlantic sea scallops (*Placopecten magellanicus*).

Interestingly, the cohorts differed subtly in their incorporation of metabolic carbon into shell $CaCO_3$ during the period while they were using maternal lipids for energy (0–7 d). This difference can be seen as the slope of the initial decrease in shell carbon signal (Fig. 3) and in the calculated fraction of metabolic carbon in the shell (Fig. 4). The 2 cohorts with the highest mean Ω_{ar} in the tank (the May cohort and the August buffered cohort) show a continuously increasing fraction of metabolic carbon with time, while the August unbuffered cohort starts with a higher fraction that decreases to a minimum incorporation of metabolic carbon at 7 d, and then has a steadily increasing metabolic contribution up to 21 d. It is important to note that the estimates include the slight difference in DIC $\delta^{13}C$ due to buffering with $NaCO_3$. Chemical buffering of water therefore appears to alter the incorporation of metabolic carbon into the shell, possibly indicating that larvae in buffered waters are less stressed, and supporting longer-term success as seen in commercial hatcheries (Barton et al. 2015) and in smaller experimental settings (Gobler et al. 2014). Lorrain et al. (2004) suggested that the ratio of respired to precipitated carbon is responsible for driving patterns of metabolic isotope incorporation in shell for *Pecten maximus*. We assumed that the calcification rate was the same for all cohorts (given that shell length did not vary), which suggests a possible metabolic depression in the August unbuffered cohort to account for the lower metabolic carbon incorporation, which could be a more subtle effect of living under slightly acidified conditions. It is also possible that length (as a measured parameter) does not reflect subtle differences in total calcification, as would be captured by shell thickness. A decoupling of shell length and thickness has been documented in mussel larvae exposed to elevated CO_2 (Gaylord et al. 2011). In general, the August cohorts were characterized by higher AFDW, especially in the first 7 d, so their higher metabolic carbon production could explain the higher metabolic carbon incorporation (Gerdes 1983, Hoegh-Guldberg & Manahan 1995).

Although conflicting data exist, it has been recognized that protein stores are important for larvae to successfully metamorphose (e.g. García-Esquivel et al. 2001), which could explain the decreasing C:N

ratios of the 2 August cohorts in later larval life — these cohorts were increasing their proportion of protein compared to lipid or carbohydrates in preparation for settlement. The coincident drawdown of lipid stores could also indicate that lipid energy reserves were being catabolized to prepare for metamorphosis. In contrast, the high lipid content in larvae at 19 d in the May cohort could be representative of slowed development due to stress; they may not yet have begun to prepare biochemically for metamorphosis when we stopped following them. Or it could be related to sampling bias, because the larvae were screened to follow only the largest of the larvae as discussed above. A final explanation for the high late-larval lipid content could be compensatory growth (Metcalfe & Monaghan 2001, discussed in Hettinger et al. 2013); the May cohort larvae may have accelerated their feeding and lipid accumulation to 'catch-up' with normal development rates.

The use of stable isotopes and the bulk biochemistry of the larvae permitted us to identify subtle changes in the larvae that do not appear to result in dramatic acute effects, but may help identify impacts during the important larval period in marine bivalves. However, we note that further studies on the ontogeny of stable isotopes in bivalve larvae would help instill greater confidence in the actual values obtained here, while the patterns found over larval development and growth were relatively consistent. Our findings illustrate that the effects of ocean acidification on marine organisms may not always be quantifiable by first-order performance characteristics such as size. Under stressful conditions, it appears that, regardless of energetic status, larvae still create very similar PDI shells, and, in fact, little difference can be detected between PDI shell grown by larvae that have fully exhausted their available energy stores (e.g. the May cohort) and those grown by larvae with ample lipid stores (e.g. the August cohorts). Our results suggest that a metric of larval health that includes an analysis of available lipids would be useful in studies of sub-lethal stress, in addition to the more traditional size-at-age measurements.

Acknowledgements. This work was supported by the National Science Foundation OCE CRI-OA No. 1041267 to G.G.W. and B.H. The authors thank the Whiskey Creek Shellfish Hatchery for providing space, larvae, and support in conducting the work within the hatchery. Jennifer McKay provided support, advice, perspective, and training for E.L.B. in running isotope samples. The authors would like to thank 3 anonymous reviewers who helped improve a previous version of this manuscript. This work was completed in partial fulfillment of a M.S. degree granted to E.L.B.

LITERATURE CITED

Bandstra L, Hales B, Takahashi T (2006) High-frequency measurements of total CO_2: method development and first oceanographic observations. Mar Chem 100:24–38

Barton A, Hales B, Waldbusser GG, Langdon C, Feely RA (2012) The Pacific oyster, *Crassostrea gigas*, shows negative correlation to naturally elevated carbon dioxide levels: implications for near-term ocean acidification effects. Limnol Oceanogr 57:698–710

Barton A, Waldbusser GG, Feely RA, Weisberg SBN and others (2015) Impacts of coastal acidification on the Pacific northwest shellfish industry and adaptation strategies implemented in response. Oceanography (Wash DC) 28:146–159

Bauer JE, Druffel ER, Wolgast DM, Griffin S, Masiello CA (1998) Distributions of dissolved organic and inorganic carbon and radiocarbon in the eastern North Pacific continental margin. Deep-Sea Res II 45:689–713

Benner R, Biddanda B, Black B, McCarthy M (1997) Abundance, size distribution, and stable carbon and nitrogen isotopic compositions of marine organic matter isolated by tangential-flow ultrafiltration. Mar Chem 57:243–263

Bochenek EA, Klinck JM, Powell EN, Hofmann EE (2001) A biochemically based model of the growth and development of *Crassostrea gigas* larvae. J Shellfish Res 20: 243–266

Dickson AG (1990) Thermodynamics of the dissociation of boric acid in synthetic seawater from 273.15 to 318.15 K. Deep-Sea Res I 37:755–766

Emmery A, Lefebvre S, Alunno-Bruscia M, Kooijman SALM (2011) Understanding the dynamics of delta C-13 and delta N-15 in soft tissues of the bivalve *Crassostrea gigas* facing environmental fluctuations in the context of Dynamic Energy Budgets (DEB). J Sea Res 66:361–371

Gallager SM, Mann R (1986) Growth and survival of larvae of *Mercenaria mercenaria* (L.) and *Crassostrea virginica* (Gmelin) relative to broodstock conditioning and lipid content of eggs. Aquaculture 56:105–121

Gallager SM, Mann R, Sasaki GC (1986) Lipid as an index of growth and viability in three species of bivalve larvae. Aquaculture 56:81–103

García-Esquivel Z, Bricelj VM, González-Gómez MA (2001) Physiological basis for energy demands and early postlarval mortality in the Pacific oyster, *Crassostrea gigas*. J Exp Mar Biol Ecol 263:77–103

Gaylord B, Hill TM, Sanford E, Lenz EA and others (2011) Functional impacts of ocean acidification in an ecologically critical foundation species. J Exp Biol 214: 2586–2594

Gazeau F, Parker LM, Comeau S, Gattuso JP and others (2013) Impacts of ocean acidification on marine shelled molluscs. Mar Biol 160:2207–2245

Gerdes D (1983) The Pacific oyster *Crassostrea gigas*: Part II. Oxygen consumption of larvae and adults. Aquaculture 31:221–231

Gobler CJ, Talmage SC (2013) Short- and long-term consequences of larval stage exposure to constantly and ephemerally elevated carbon dioxide for marine bivalve populations. Biogeosciences 10:2241–2253

Gobler CJ, DePasquale EL, Griffith AW, Baumann H (2014) Hypoxia and acidification have additive and synergistic negative effects on the growth, survival, and metamorphosis of early life stage bivalves. PLOS ONE 9:e83648

Hedges JI, Stern JH (1984) Carbon and nitrogen determina-

tions of carbonate-containing solids. Limnol Oceanogr 29:657–663

Hettinger A, Sanford E, Hill TM, Russell AD and others (2012) Persistent carry-over effects of planktonic exposure to ocean acidification in the Olympia oyster. Ecology 93:2758–2768

Hettinger A, Sanford E, Hill TM, Lenz EA, Russell AD, Gaylord B (2013) Larval carry-over effects from ocean acidification persist in the natural environment. Glob Chang Biol 19:3317–3326

His E, Maurer D (1988) Shell growth and gross biochemical composition of oyster larvae (*Crassostrea gigas*) in the field. Aquaculture 69:185–194

His E, Robert R, Dinet A (1989) Combined effects of temperature and salinity on fed and starved larvae of the Mediterranean mussel *Mytilus galloprovincialis* and the Japanese oyster *Crassostrea gigas*. Mar Biol 100:455–463

His E, Seaman MNL, Beiras R (1997) A simplification the bivalve embryogenesis and larval development bioassay method for water quality assessment. Water Res 31: 351–355

Hoegh-Guldberg O, Manahan D (1995) Coulometric measurement of oxygen consumption during development of marine invertebrate embryos and larvae. J Exp Biol 198: 19–30

Kennedy V (1996) Biology of larvae and spat. In: The eastern oyster : *Crassostrea virginica*. Maryland Sea Grant College, College Park, MD, p 371–421

Kniprath E (1981) Ontogeny of the molluscan shell field: a review. Zool Scr 10:61–79

Kroeker KJ, Kordas RL, Crim RN, Singh GG (2010) Meta-analysis reveals negative yet variable effects of ocean acidification on marine organisms. Ecol Lett 13: 1419–1434

Kroeker KJ, Kordas RL, Crim R, Hendriks IE and others (2013) Impacts of ocean acidification on marine organisms: quantifying sensitivities and interaction with warming. Glob Chang Biol 19:1884–1896

Kudo M, Kameda J, Saruwatari K, Ozaki N, Okano K, Nagasawa H, Kogure T (2010) Microtexture of larval shell of oyster, *Crassostrea nippona*: a FIB-TEM study. J Struct Biol 169:1–5

Kurihara H (2008) Effects of CO_2-driven ocean acidification on the early developmental stages of invertebrates. Mar Ecol Prog Ser 373:275–284

Labarbera M (1974) Calcification of first larval shell of *Tridacna–Squamosa* (Tridacnidae–Bivalvia). Mar Biol 25: 233–238

Lorrain A, Paulet YM, Chauvaud L, Dunbar R, Mucciarone D, Fontugne M (2004) $\delta^{13}C$ variation in scallop shells: increasing metabolic carbon contribution with body size? Geochim Cosmochim Acta 68:3509–3519

Maberly SC, Raven JA, Johnston AM (1992) Discrimination between ^{12}C and ^{13}C by marine plants. Oecologia 91: 481–492

Maeda-Martinez A (1987) The rates of calcium deposition in shells of molluscan larvae. Comp Biochem Physiol A 86: 21–28

Marin F, Luquet G, Marie B, Medakovic D (2008) Molluscan shell proteins: primary structure, origin, and evolution. In: Schatten GP (ed) Current topics in developmental biology, Vol 80. Elsevier Academic Press Inc, San Diego, CA, p 209–276

Massapina C, Joaquim S, Matias D, Devauchelle N (1999) Oocyte and embryo quality in *Crassostrea gigas* (Portuguese strain) during a spawning period in Algarve, South Portugal. Aquat Living Resour 12:327–333

Matias D, Joaquim S, Ramos M, Sobral P, Leitão A (2011) Biochemical compounds' dynamics during larval development of the carpet-shell clam (Linnaeus, 1758): effects of monospecific diets and starvation. Helgol Mar Res 65:369–379

McConnaughey TA, Gillikin DP (2008) Carbon isotopes in mollusk shell carbonates. Geo-Mar Lett 28:287–299

McConnaughey TA, Burdett J, Whelan JF, Paull CK (1997) Carbon isotopes in biological carbonates: respiration and photosynthesis. Geochim Cosmochim Acta 61:611–622

McFarland K, Donaghy L, Volety A (2013) Effect of acute salinity changes on hemolymph osmolality and clearance rate of the non-native mussel, *Perna viridis*, and the native oyster, *Crassostrea virginica*, in Southwest Florida. Aquat Invasions 8:299–310

Medakovic D (2000) Carbonic anhydrase activity and biomineralization process in embryos, larvae and adult blue mussels *Mytilus edulis* L. Helgol Mar Res 54:1–6

Metcalfe NB, Monaghan P (2001) Compensation for a bad start: Grow now, pay later? Trends Ecol Evol 16:254–260

Millero FJ (2010) Carbonate constants for estuarine waters. Mar Freshw Res 61:139–142

Moran AL, Manahan DT (2004) Physiological recovery from prolonged starvation in larvae of the Pacific oyster *Crassostrea gigas*. J Exp Mar Biol Ecol 306:17–36

Moran AL, McAlister JS (2009) Egg size as a life history character of marine invertebrates: Is it all it's cracked up to be? Biol Bull 216:226–242

Mouëza M, Gros O, Frenkiel L (2006) Embryonic development and shell differentiation in *Chione cancellata* (Bivalvia, Veneridae): an ultrastructural analysis. Invertebr Biol 125:21–33

Mount AS, Wheeler AP, Paradkar RP, Snider D (2004) Hemocyte-mediated shell mineralization in the eastern oyster. Science 304:297–300

Mucci A (1983) The solubility of calcite and aragonite in seawater at various salinities, temperatures, and one atmosphere total pressure. Am J Sci 283:780–799

Muranaka M, Lannan J (1984) Broodstock management of *Crassostrea gigas*: environmental influences on broodstock conditioning. Aquaculture 39:217–228

Owen EF, Wanamaker AD Jr, Feindel SC, Schöne BR, Rawson PD (2008) Stable carbon and oxygen isotope fractionation in bivalve (*Placopecten magellanicus*) larval aragonite. Geochim Cosmochim Acta 72:4687–4698

Palmer AR (1992) Calcification in marine mollusks — How costly is it? Proc Natl Acad Sci USA 89:1379–1382

Pan TCF, Applebaum SL, Manahan DT (2015) Experimental ocean acidification alters the allocation of metabolic energy. Proc Natl Acad Sci USA 112:4696–4701

Parker LM, Ross P, O'Connor W, Pörtner H, Scanes E, Wright J (2013) Predicting the response of molluscs to the impact of ocean acidification. Biology (Basel) 2:651–692

Pechenik JA (2006) Larval experience and latent effects — metamorphosis is not a new beginning. Integr Comp Biol 46:323–333

Rau G, Riebesell U, Wolf-Gladrow D (1996) A model of photosynthetic ^{13}C fractionation by marine phytoplankton based on diffusive molecular CO_2 uptake. Mar Ecol Prog Ser 133:275–285

Raven JA, Johnston AM, Kübler JE, Korb R and others (2002) Mechanistic interpretation of carbon isotope discrimination by marine macroalgae and seagrasses. Funct Plant Biol 29:355–378

Ries JB (2011) Skeletal mineralogy in a high-CO_2 world. J Exp Mar Biol Ecol 403:54–64

Ries JB, Cohen AL, McCorkle DC (2009) Marine calcifiers exhibit mixed responses to CO_2-induced ocean acidification. Geology 37:1131–1134

Romanek CS, Grossman EL, Morse JW (1992) Carbon isotopic fractionation in synthetic aragonite and calcite: effects of temperature and precipitation rate. Geochim Cosmochim Acta 56:419–430

Tang B, Liu B, Wang G, Zhang T, Xiang J (2006) Effects of various algal diets and starvation on larval growth and survival of *Meretrix meretrix*. Aquaculture 254:526–533

Timmins-Schiffman E, O'Donnell MJ, Friedman CS, Roberts SB (2013) Elevated pCO_2 causes developmental delay in early larval Pacific oysters, *Crassostrea gigas*. Mar Biol 160:1973–1982

Uriarte I, Farias A, Hernandez J, Schafer C, Sorgeloos P (2004) Reproductive conditioning of Chilean scallop (*Argopecten purpuratus*) and the Pacific oyster (*Crassostrea gigas*): effects of enriched diets. Aquaculture 230: 349–357

Verardo DJ, Froelich PN, McIntyre A (1990) Determination of organic carbon and nitrogen in marine sediments using the Carlo Erba NA-1500 Analyzer. Deep-Sea Res Part I 37:157–165

Waldbusser GG, Salisbury JE (2014) Ocean acidification in the coastal zone from an organism's perspective: multiple system parameters, frequency domains, and habitats. Ann Rev Mar Sci 6:221–247

Waldbusser GG, Bergschneider H, Green MA (2010) Size-dependent pH effect on calcification in post-larval hard clam *Mercenaria* spp. Mar Ecol Prog Ser 417:171–182

Waldbusser GG, Brunner EL, Haley BA, Hales B, Langdon CJ, Prahl FG (2013) A developmental and energetic basis linking larval oyster shell formation to acidification sensitivity. Geophys Res Lett 40:2171–2176

Waldbusser GG, Hales B, Langdon CJ, Haley BA and others (2015a) Saturation-state sensitivity of marine bivalve larvae to ocean acidification. Nat Clim Change 5:273–280

Waldbusser GG, Hales B, Langdon CJ, Haley BA and others (2015b) Ocean acidification has multiple modes of action on bivalve larvae. PLOS ONE 10:e0128376

Waldbusser GG, Hales B, Haley BA (2016a) Calcium carbonate saturation state: on myths and this or that stories. ICES J Mar Sci 73:563–568

Waldbusser GG, Gray MW, Hales B, Langdon CJ and others (2016b) Slow shell building, a trait for resiliency to acute ocean acidification impacts. Limnol Oceanogr, doi: 10.1002/lno.10348

Walker BD, McCarthy MD (2012) Elemental and isotopic characterization of dissolved and particulate organic matter in a unique California upwelling system: importance of size and composition in the export of labile material. Limnol Oceanogr 57:1757–1774

Waller TR (1981) Functional morphology and development of veliger larvae of the European oyster. Smithson Contrib Zool 328:1–70

Weiss IM, Tuross N, Addadi L, Weiner S (2002) Mollusc larval shell formation: amorphous calcium carbonate is a precursor phase for aragonite. J Exp Zool 293:478–491

Whiting MC, McIntire CD (1985) An investigation of distributional patterns in the diatom flora of Netarts Bay, Oregon, by correspondence analysis. J Phycol 21:655–661

Widdows J (1991) Physiological ecology of mussel larvae. Aquaculture 94:147–163

Yokoo N, Suzuki M, Saruwatari K, Aoki H, Watanabe K, Nagasawa H, Kogure T (2011) Microstructures of the larval shell of a pearl oyster, *Pinctada fucata*, investigated by FIB-TEM technique. Am Mineral 96:1020–1021

Editorial responsibility: James McClintock, Birmingham, Alabama, USA

Submitted: November 26, 2015; Accepted: July 5, 2016
Proofs received from author(s): August 2, 2016